

Paper No. E-7  
Prepared for  
Cryogenic Engr. Conference  
Boulder, Colorado  
Aug. 19-21, 1963

N65-88801

~~X68-15588~~

CODE-2A

(NASA TMK-50517)

CAVITATION AND EFFECTIVE LIQUID TENSION OF NITROGEN IN A  
HYDRODYNAMIC CRYOGENIC TUNNEL

By Robert S. Ruggeri and Thomas F. Gelder [1963] 17p 6x9

Lewis Research Center  
National Aeronautics and Space Administration  
Cleveland, Ohio

ABSTRACT

15588

Cavitation studies with liquid nitrogen, and with water for comparison, were conducted to determine the minimum local pressures at the threshold of visible incipient cavitation. Cavitation was induced in a transparent venturi section that had a 1.377-in. throat diameter and was mounted in a small close-return tunnel. At incipient cavitation, minimum local pressures that were considerably less than vapor pressure were always obtained with both liquids; this pressure difference is called effective liquid tension. Such effective tensions in liquid nitrogen ranged as high as 60 ft of head at a stream velocity of 55 ft/sec, and those in water rose to 24 ft of head at 45 ft/sec. Temperatures and pressures measured within regions of well-developed cavitation were in thermodynamic equilibrium but were less than free-stream values of temperature and vapor pressure. In water, these effects were small. In nitrogen, temperature and vapor pressure depressions that were as high as 3° F and 9 ft of head, respectively, were obtained.

Available to NASA Offices and  
NASA Centers Only.

E-2111

Paper No. E-7  
Prepared for  
Cryogenic Engr. Conference  
Boulder, Colorado  
Aug. 19-21, 1963

## CAVITATION AND EFFECTIVE LIQUID TENSION OF NITROGEN IN A HYDRODYNAMIC CRYOGENIC TUNNEL

By Robert S. Ruggeri and Thomas F. Gelder

Lewis Research Center  
National Aeronautics and Space Administration  
Cleveland, Ohio

### INTRODUCTION

Cavitation may be described as the local vaporization of a liquid brought about by reductions in pressure due to changes in flow velocity. For the most part, cavitation is undesirable. It is damaging, often to the point of destruction. It is noisy, usually is accompanied by vibration, and generally degrades the flow pattern. It is generally assumed that cavitation will occur if the local minimum pressure within a flowing system is reduced to the fluid vapor pressure. Also, the pressure within a cavity, or cavitated region, is usually thought to be at the vapor pressure corresponding to stream liquid temperature. These assumptions are not always valid (refs. 1 to 6). In fact, recent experimental evidence that shows to what extent these assumptions may be invalid (for a particular model) constitutes the subject of the present paper.

First, it is shown that liquids can flow cavitation free through pressure regions that are significantly less than saturation vapor pressure corresponding to free-stream liquid temperature. For this condition, the liquid is locally in a thermodynamically metastable state of superheat, and as such, the flowing liquid can be expected to sustain these unusually

low pressures only for relatively short periods of time. The maximum decrement of local pressure relative to stream vapor pressure that existed at, or just prior to, incipient cavitation is called, for engineering purposes herein, effective liquid tension. Effective tension may be viewed as a pressure difference tending to rupture, or cavitate, the liquid.

Second, from a brief study of the temperature and pressure effects of the phase change that occurs during cavitation, (so-called thermodynamic effects) it is shown that temperatures and pressures within a cavitated region can be appreciably less than free-stream values of temperature and vapor pressure. Such effects appear to be significant factors affecting pump performance and have been related to the different properties of the liquids being considered (refs. 4 to 6).

The present study was conducted at the NASA Lewis Research Center where a small cavitation tunnel facility with liquid nitrogen as the test fluid was used. Water, studied previously in the same facility, is used as a reference liquid for comparative purposes. This investigation is aimed at obtaining a better understanding of cavitation phenomena and thereby establishing firmer design procedures for high-performance lightweight pumps for rockets and spacecraft.

#### APPARATUS AND PROCEDURE

Cavitation was induced on the walls of a transparent venturi section mounted in the upper leg of a small closed-return tunnel. For liquid-nitrogen operation, the entire tunnel is submerged in a liquid-nitrogen bath, which acts as a heat sink to remove heat imparted to the tunnel

liquid by the environment and by the circulating pump. A schematic drawing of the complete tunnel-bath arrangement is presented in figure 1. The tunnel is designed to accomodate 12-in.-long test sections with maximum inlet diameters of 1.743 in.. The tunnel is fabricated of aluminum (6061-T6) to ensure good heat transfer between tunnel and bath liquids. Liquid capacity of the tunnel is about 10 gal (U.S.). The 15-hp variable-speed pump-drive system provides operational flow velocities from about 17 to 85 ft/sec at the test section inlet. The centrifugal pump is a commercially available unit designed to handle cryogenic liquids. For a constant tunnel velocity, the extent of cavitation induced in the test section is controlled by varying the gas pressure in the expansion chamber.

The cryogenic bath surrounding the tunnel is fabricated from 304 stainless steel and is externally insulated with 1/2-in.-thick composition corkboard bonded directly to the metal. The bath has about a 70-gal capacity. Two side windows and one top window (all of 2-in.-thick Lucite) are provided for viewing, lighting, and photographing. Bath liquid level is controlled automatically, and boiling in the bath may be temporarily suppressed by valving off the vent line. The tunnel liquid does not boil because it is normally subcooled by pressurization with dry nitrogen or helium gas. No flexible joints or bellows are employed in either the bath or the tunnel loop.

The venturi test section (fig. 2) is a machined Lucite tube mated to aluminum end flanges by means of shrink fits. It consists of a constant diameter approach section (1.743 in. diam.), which is reduced to  $1\frac{3}{8}$ -in. diam. at the throat by means of a slightly modified quarter-round constriction. This quarter-round shape generates a wall pressure distribution

with a deep but narrow minimum pressure valley that exposes the flowing to low pressures for very short times. The constant diameter throat is followed by a shallow-angled diffuser to minimize flow separation.

## RESULTS

### Noncavitating Pressure Distribution

The noncavitating pressure distribution for the venturi is shown in figure 3. The data are plotted in terms of a pressure coefficient  $C_p$  as a function of the axial distance from the minimum pressure point.  $C_p$  is conventionally defined as the difference between the local wall and free-stream static-pressure head ( $h_x - h_o$ ) divided by the velocity head  $V_o^2/2g$ . Free-stream conditions are measured in the approach section about 1 in. upstream from the quarter round. The solid line (fig. 3) represents a computed ideal flow solution. The dashed line represents experimental data obtained with nitrogen and water in the cavitation tunnel and from a scaled-up aerodynamic model studied in a large wind tunnel. The experimental results shown are all for a Reynolds number of about 600,000. The data for the various fluids are in good agreement, especially in the critical minimum pressure region. The experimental pressure distribution shown here is assumed to apply at incipient cavitation, or more exactly, to the single-phase liquid condition just prior to the first visible cavitation.

For the present study, the most important part of the pressure distribution curve is the location and value of  $C_p$  at the point of minimum pressure  $C_{p,min}$ , since it is at this point that cavitation can first be expected to occur. The minimum pressure point is located on the quarter

round at  $66^\circ$  of arc measured from the approach section wall, and its location did not change over the range of free-stream velocities studied.

#### Observations of Cavitation

A photograph showing typical incipient cavitation in water is presented in figure 4. The start of the quarter round can be noted by the dark vertical line and a burst of cavitation can be seen a short distance downstream from this point. Incipient cavitation bursts form almost instantaneously and usually last but a few milliseconds. There may then be several seconds of cavity-free flow before another burst occurs. The leading edge of the cavities was always located very near the point of minimum pressure, that is, the  $66^\circ$  point. For small extents of cavitation, the cavities appear as individual streamers (as shown) which form and collapse very rapidly. It is rare that the life of a single streamer will persist for 0.001 sec.

Once cavitation occurs, a further reduction in free-stream pressure simply produces larger amounts of cavitation with the individual streamers merging to form a thin annulus of vapor cavities that have a well-defined leading edge. For the present venturi, cavitation is always confined to a thin ring adjacent to the wall, since wall pressures are lower than pressures further into the stream. With water, the trailing edge, or collapsing region, of cavitation was rather sharp and the condensing vapor bubbles did not persist long before complete collapse occurred.

A photograph showing typical liquid nitrogen cavitation is presented in figure 5. The nitrogen cavitation shown is for a condition that is slightly in excess of the incipient level. Even so, marked differences

between cavitation in nitrogen and that in water are apparent. For all degrees of nitrogen cavitation studied, the process was much less violent than it was for water. In general, rates of cavity formation in nitrogen appeared to be much slower than those in water, whereas rates of collapse may be comparable for similar axial pressure gradients. At the highest stream velocity studied, incipient cavitation in nitrogen tended to resemble incipient cavitation in water, although for nitrogen the axial pressure gradients through the venturi were much steeper.

#### Effective Liquid Tension

The actual technique used in evaluating effective liquid <sup>tension</sup> can be more easily described with the aid of figure 6 which is a magnified plot of figure 3 showing only the low pressure region of the pressure distribution curve. For all noncavitating conditions,  $C_p$  is independent of pressure level; and for the range of speeds studied, it is essentially independent of Reynolds number. By measuring free-stream pressure and velocity, the minimum absolute pressure  $h_{min}$  on the model may be computed from the known experimental value of  $C_{p,min}$  ( $C_{p,min} = (h_{min} - h_o) / V_o^2 / 2g$ ). Specifically, the value of  $h_{min}$  at incipient cavitation was obtained as follows: Starting from a noncavitating condition at a fixed tunnel speed  $V_o$ , the tunnel pressure  $h_o$  was slowly reduced until random bursts of incipient cavitation were observed on the model. At this condition,  $h_o$ ,  $V_o$ , and liquid temperature were measured. The absolute value of minimum pressure was then calculated and compared with the vapor pressure corresponding to free-stream liquid temperature to determine effective liquid tensions, if any. The results obtained for nitrogen and water are shown in figure 7.

Effective liquid tension, defined as the minimum pressure  $h_{\min}$  minus stream vapor pressure  $h_v$ , in feet of liquid, is shown in figure 7 plotted as a function of free-stream velocity. The data show that appreciable effective tensions were always obtained in both liquid nitrogen and water, where the values obtained in nitrogen were about twice those in water for a given stream velocity. Values of effective tension increase with increasing stream velocity, apparently because the time that the liquids are exposed to low pressure decreases as stream velocity increases. The water data were obtained with demineralized, tap, and distilled water over a range of air content from 6.7 to 125 percent of saturation (at 85°F and atmospheric pressure). Thus, the type of water or its air content had no effect on absolute values of minimum pressure existing at incipient conditions. For water, effective tension values range from about 4 ft of head at low speed to about 24 ft or 11 psi at 45 ft/sec. In nitrogen, the effective liquid tension ranged to as much as 60 ft of head, or about 21 psi, at a stream velocity of 55 ft/sec.

#### Effects of Cavitation on Local Temperatures and Pressures

Although liquid temperatures are uniform throughout the venturi in noncavitating flow, the effective tensions obtained at incipient cavitation (fig. 7) indicate that the fluid is locally superheated and thus not in a state of thermodynamic equilibrium. When the fluid ruptures or cavitates, a phase change occurs because the voids rapidly fill with vapor. Vapor generation requires heat of vaporization, which must be drawn from the surrounding liquid. This should result in a cooling of the vapor-liquid



interface and a reduction in temperature around and within the cavity. If conditions within the cavity are in thermodynamic equilibrium, then a definite pressure drop should accompany the drop in temperature.

From the standpoint of predicting pump performance for different liquids, it is this lowered pressure within the cavitated region that is of primary importance. In order to evaluate these temperature and pressure effects, a fixed amount of cavitation was generated in nitrogen and water after which the stabilized temperatures and pressures within the cavitated region were measured. Typical results are shown in figure 8.

The plot in figure 8 shows typical pressure variations within the cavitated nitrogen region as a function of axial distance. The amount of cavitation existing at the time the data were taken is sketched at the bottom of the figure; well-developed cavitation existed for about 2 in. at which point the collapse region began. The solid curve through the open symbols represents measured pressures along the venturi, while the horizontal line represents vapor pressure corresponding to free-stream temperature ( $140.0^{\circ}$  R). In the cavitated region (first 2 in.), the measured pressures are all less than vapor pressure corresponding to free-stream liquid temperature. Also, the start of the collapse region of cavitation coincides closely with the point at which the curve of measured pressures crosses the stream vapor pressure line. Further downstream, the pressures increase and approach the noncavitating values (except for head losses) shown by the dashed line.

The solid symbols represent values of saturation vapor pressure, which correspond to the measured temperatures shown in parentheses. These temperatures ranged from  $138.6^{\circ}$  to  $139.9^{\circ}$  R. The vapor pressures obtained from these temperature measurements agree with the local static pressures measured directly; thus, thermodynamic equilibrium appears to exist within the cavity. The pressure within the cavity thus corresponds to the vapor pressure based on a locally reduced or depressed temperature and not on free-stream temperature as might be assumed if thermodynamic effects were not considered. Note that for nitrogen, a  $1.4^{\circ}$  temperature depression corresponds to a 4 ft drop in head of vapor pressure. The value of minimum pressure shown (40 ft of liquid nitrogen abs) is greater than that which existed at incipient conditions (33 ft abs or 11 ft or effective liquid tension - see fig. 7). A change from the thermodynamically metastable state of the liquid at, or just prior to, incipient cavitation to one of thermodynamic equilibrium with cavitation thus produces a discontinuity in the value of minimum pressure.

Temperature and head depression values were found to increase with both tunnel speed and extent of cavitation. At 45 ft/sec, the temperature depressions in nitrogen were about  $3^{\circ}$  F, which is equivalent to 9 ft of vapor-pressure head depression. In comparison to liquid nitrogen, the temperature and pressure effects in water at room temperature were quite small. Measured temperature depressions ranged from about  $0.1^{\circ}$  to  $0.3^{\circ}$  F. Changes in vapor pressure due to these small temperature depressions are insignificant; thus, pressures within the cavitated region in water

correspond essentially to vapor pressure based on free-stream temperature. On a plot such as figure 8, the pressures in the cavitated region for water would follow the free-stream vapor pressure line and then begin to rise to the noncavitating values at the start of the collapse region.

There are indications that with liquid hydrogen, the temperature depression in a cavitated region may be as great as or greater than those measured in nitrogen; in this case the depressed vapor pressure head becomes quite appreciable and may reach the order of 100 ft of liquid or more.

#### SUMMARY OF RESULTS

Experimental studies of liquid nitrogen and water cavitation in a tunnel-mounted venturi yielded the following principal results:

1. For both liquids, local minimum wall pressures, which were significantly less than vapor pressure corresponding to free-stream temperature, were always obtained in the single-phase liquid (superheated) at, or just prior to, incipient cavitation. These effective liquid tensions in nitrogen ranged to as much as 60 ft of head (21 psi) and those in water to 24 ft (11 psi).
2. Within regions of well-developed cavitation, measured temperatures and pressures were in thermodynamic equilibrium but were less than free-stream values of temperature and vapor pressure. In nitrogen, temperature and vapor pressure depressions of as much as  $3^{\circ}$  F and 9 ft of head, respectively, were obtained. These effects increased with increased stream velocity and extent of cavitation. In water, these effects were quite small.

REFERENCES

1. Ruggeri, R. S., and Gelder, T. F.: Effects of Air Content and Water Purity on Liquid Tension at Incipient Cavitation in Venturi Flow. NASA TN D-1459, 1963.
2. Ziegler, G.: Tensile Stresses in Flowing Water. Cavitation in Hydrodynamics - Proc. of Symposium, Nat. Phys. Lab., Sept. 14-17, 1955.
3. Crump, S. F.: Determination of Critical Pressures for the Inception of Cavitation in Fresh and Sea Water as Influenced by Air Content of Water. Rep. 575, David W. Taylor Model Basin, Oct. 1949.
4. Stahl, H. A., and Stepanoff, A. J.: Thermodynamic Aspects of Cavitation in Centrifugal Pumps. Trans. ASME, 78, 1691 (1956).
5. Jacobs, R. B.: Prediction of Symptoms of Cavitation. Jour. of Res. Nat. Bur. of Standards, vol. 65C, no. 3, July-Sept. 1961.
6. Wilcox, W. W., Meng, P. R., and Davis, R. L.: Performance of an Inducer-Impeller Combination at or near Boiling Conditions for Liquid Hydrogen. Paper presented at Cryogenic Eng. Conf., Los Angeles, Calif., Aug. 14-16, 1962.

E-2111

Figure Legend

Figure 1. - Cryogenic cavitation tunnel facility.

---

Figure 2. - Sketch of venturi test section.

---

Figure 3. - Noncavitating pressure head distribution.

---

Figure 4. - Typical incipient cavitation in water. Free-stream velocity, 28 ft/sec; temperature, 89° F; demineralized water 42 percent saturated with air.

---

Figure 5. - Cavitation in liquid nitrogen. Free-stream velocity; 27 ft/sec; temperature, 140.4° R.

---

Figure 6. - Magnified plot of low pressure region.

---

Figure 7. - Effective liquid tension for nitrogen and water.

---

Figure 8. - Head and temperature depressions within nitrogen cavity.

---

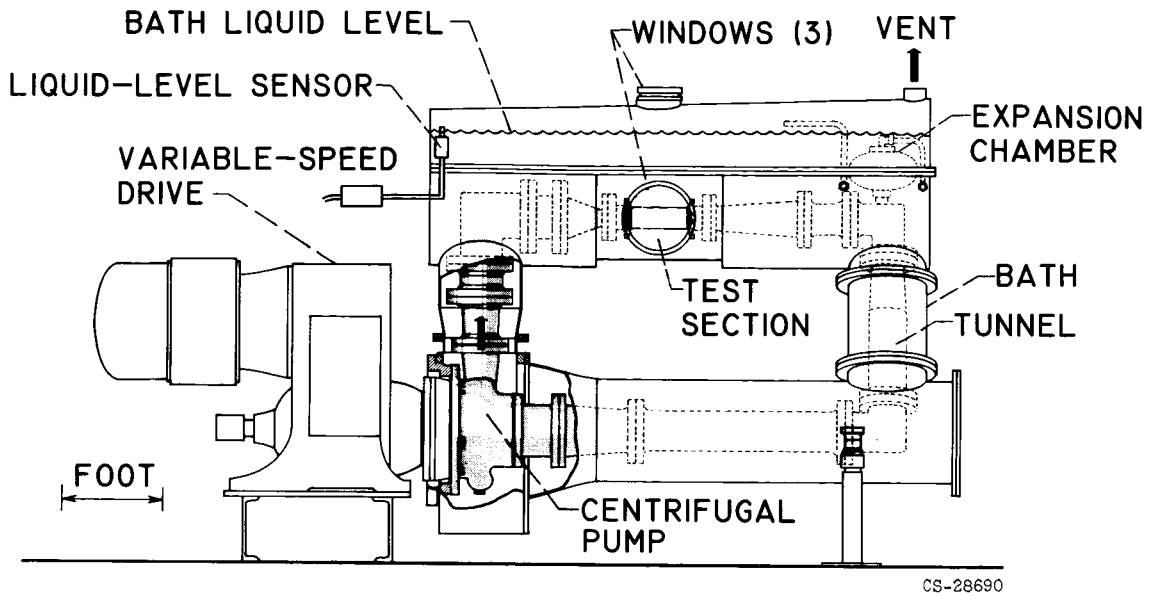


Figure 1. - Cryogenic cavitation tunnel facility.

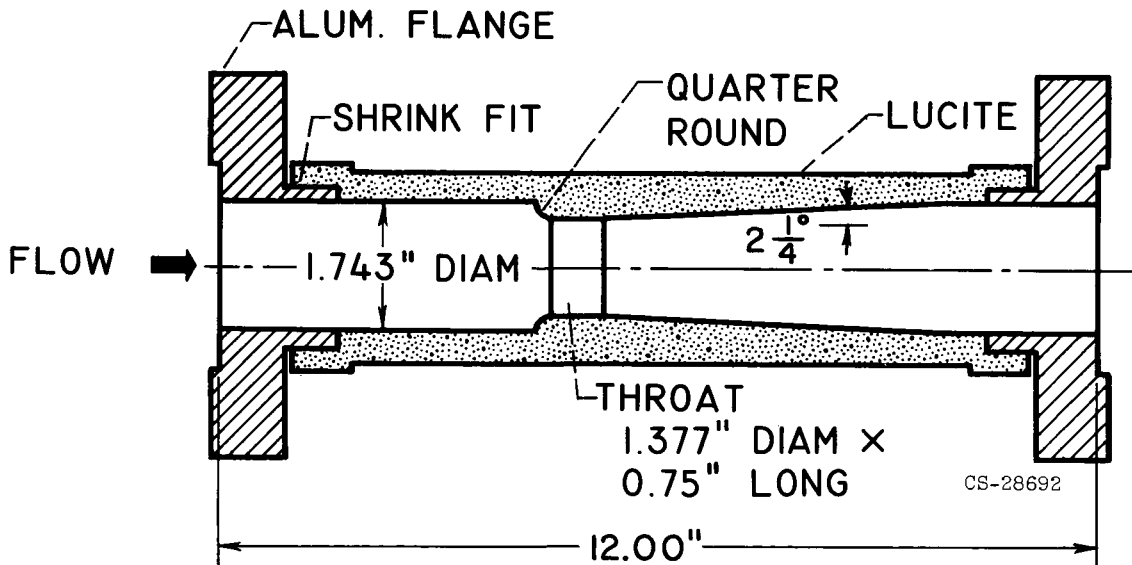


Figure 2. - Sketch of Venturi test section.

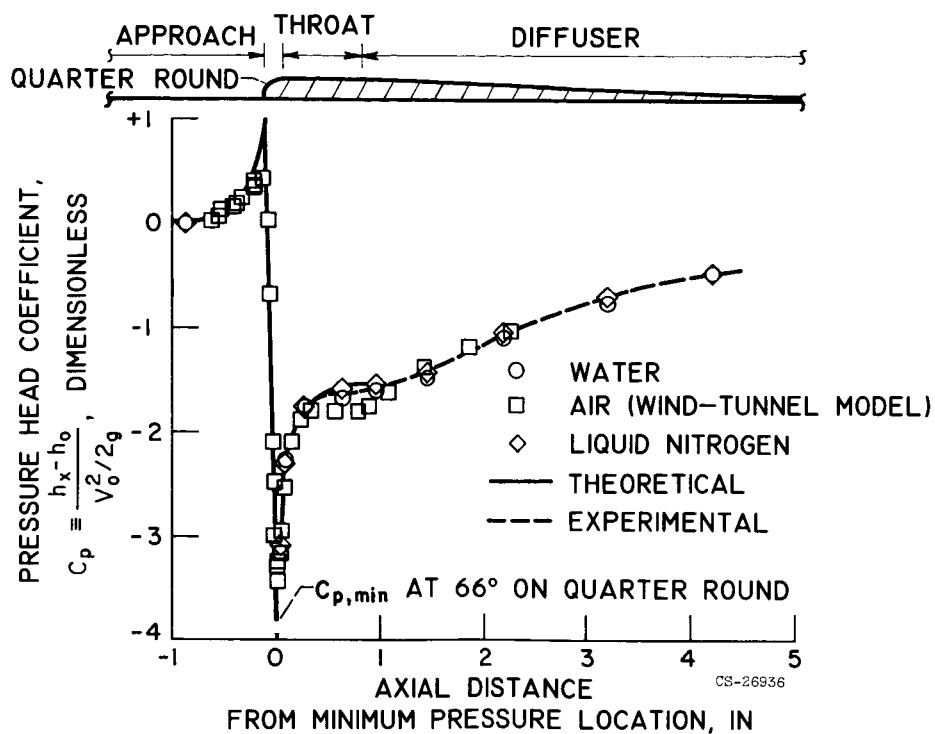


Figure 3. - Noncavitating pressure head distribution.

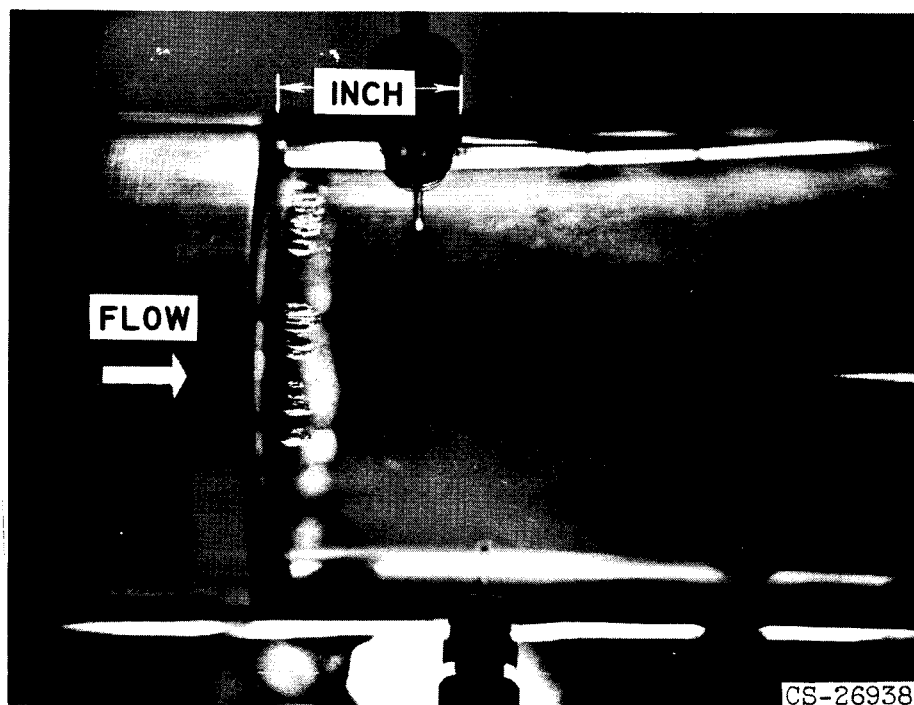


Figure 4. - Typical incipient cavitation in water.  
 Free-stream velocity, 28 ft/sec; temperature, 89°  
 F; demineralized water 42% saturated with air.

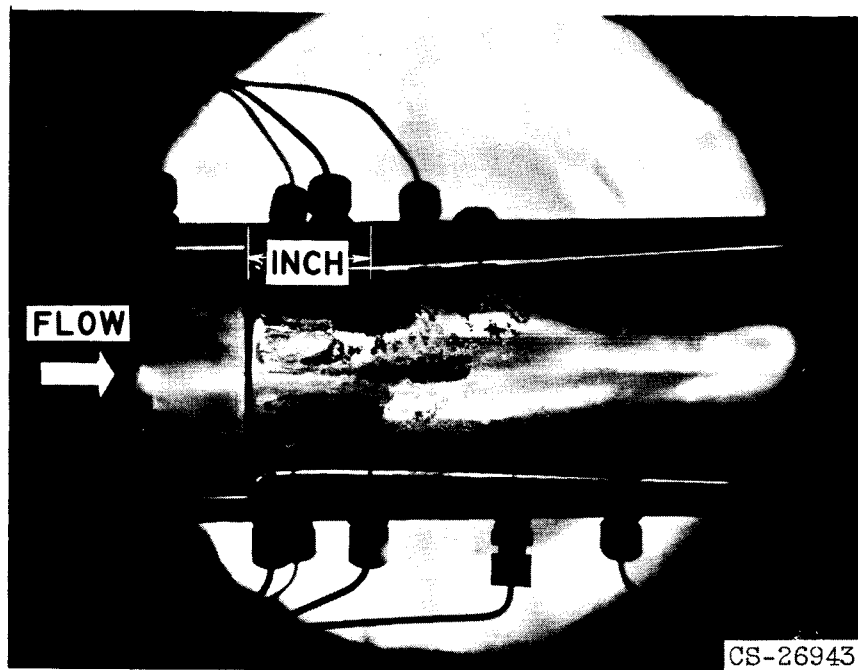


Figure 5. - Cavitation in liquid nitrogen.  
Free-stream velocity, 27 ft/sec; temperature, 140.4° R.

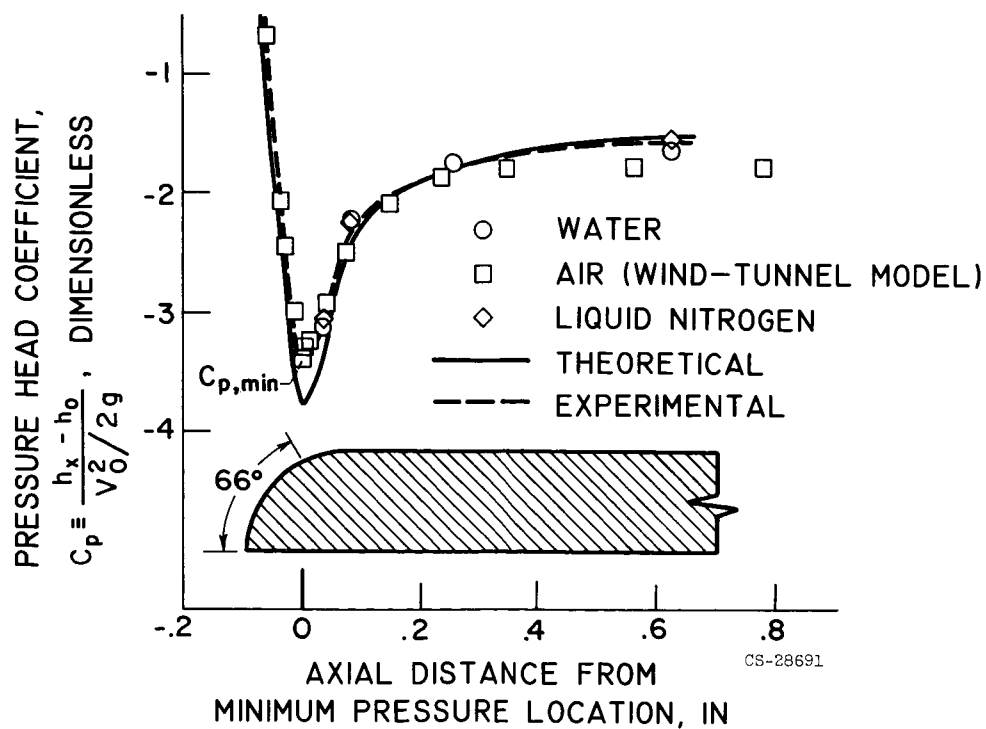


Figure 6. - Magnified plot of low pressure region.



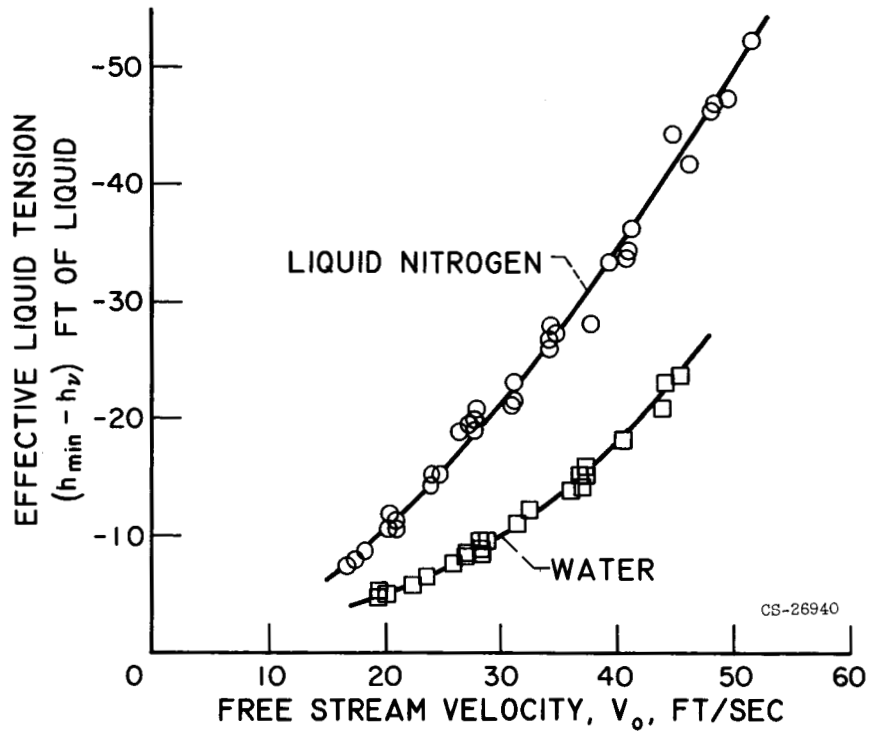


Figure 7. - Effective liquid tension for nitrogen and water.

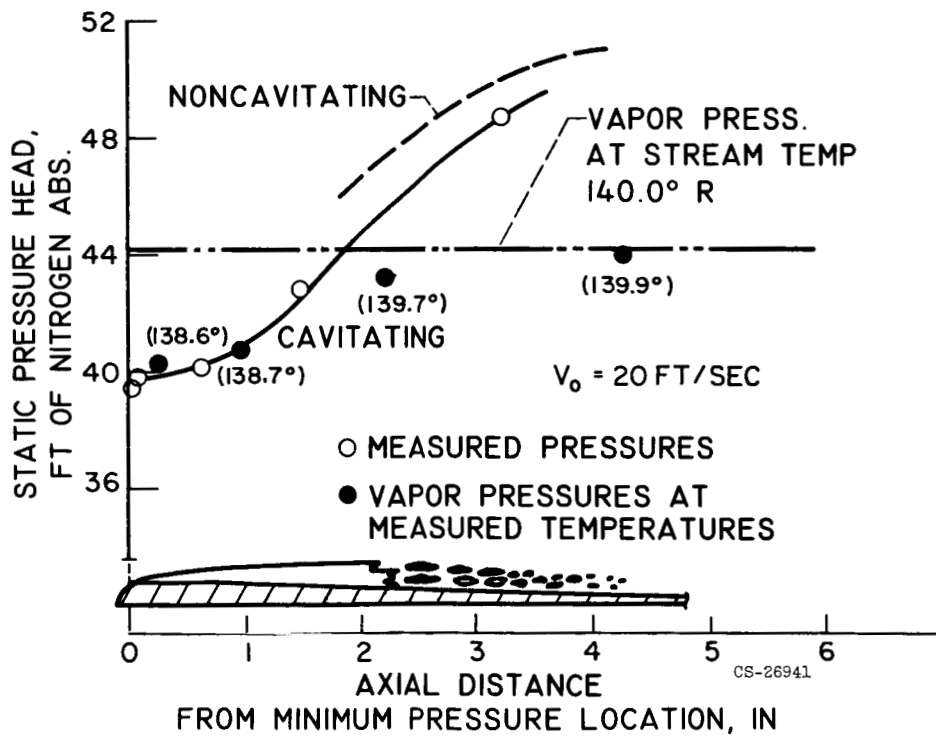


Figure 8. - Head and temperature depressions within nitrogen cavity.